Mol. Cryst. Liq. Cryst., Vol. 434, pp. 259/[587]–270/[598], 2005

ISSN: 1542-1406 print/1563-5287 online
DOI: 10.1080/15421400590957288

Taylor & Francis
Taylor & Francis Group

Lyotropic Chromonic Liquid Crystals for Biological Sensing Applications

S. V. Shiyanovskii
O. D. Lavrentovich
Chemical Physics Interdisciplinary Program and Liquid Crystal Institute, Kent State University, Kent, Ohio

T. Schneider
T. Ishikawa
Chemical Physics Interdisciplinary Program, Kent State University, Kent, Ohio

I. I. Smalyukh
Liquid Crystal Institute, Kent State University, Kent, Ohio

C. J. Woolverton
Department of Biological Sciences, Kent State University, Kent, Ohio

G. D. Niehaus
Department of Physiology, Northeastern Ohio Universities College of Medicine, Rootstown, Ohio

K. J. Doane
Department of Anatomy, Northeastern Ohio Universities College of Medicine, Rootstown, Ohio

We describe director distortions in the nematic liquid crystal (LC) caused by a spherical particle with tangential surface orientation of the director and show that light transmittance through the distorted region is a steep function of the particle's size. The effect allows us to propose a real-time microbial sensor based on a lyotropic chromonic LC (LCLC) that detects and amplifies the presence of immune complexes. A cassette is filled with LCLC, antibody, and antigen-bearing particles. Small and isolated particles cause no macroscopic distortions of the uniformly aligned LCLC. Upon antibody-antigen binding, the growing immune complexes

Address correspondence to S. V. Shiyanovskii, Liquid Crystal Institute and Department of Biological Sciences, Kent State University, Kent, Ohio 44242, USA. E-mail: svshiyan@lci.kent.edu

Keywords: biosensor; chromonics; liquid crystal

INTRODUCTION

There is a growing interest in using the nematic liquid crystals (NLCs) in biological sensors as the medium that amplifies the molecular- and submicron-scale reactions such as ligand-receptor binding to the macro-scale accessible for optical detection [1–7]. Abbott *et al.* proposed a technique based on anchoring transition at the nematic surface [1]. The liquid crystal is aligned in the cell with substrates coated with gold films and surface-bound antigens (receptors). If there is an antibody in the system that binds to the receptors, the LC-receptor interface is replaced with the LC-antibody interface at which the director orientation might be different from the orientation at the LC-receptor interface. The changes in the director configuration can be detected by optical means. There are two limitations. First, the proper alignment of LC at the substrates with receptors is challenging [5], as the receptors should function simultaneously as the antibody-specific sites and as aligning agents for the LC. Second, the LCs capable of anchoring transitions are usually of the thermotropic (solvent-free) oil-like type [8], practically immiscible with water which is the typical carrier of many biological species. The thermotropic LCs are often toxic [9]. The alternative class of LCs, the lyotropic LCs formed by aqueous solutions of amphiphilic (surfactant) molecules [8] are hard to use, because, first, the surfactants often alter the integrity of the antigen-presenting membrane surfaces of cells, and second, the surfactant molecules prefer to align perpendicularly to interfaces making the anchoring transitions difficult to induce.

In this work we describe a physical background of a different sensor technique, in which the director distortions occur in the bulk of the LC. The antigen-bearing agents (particles or microbes) and the corresponding antibodies are free to move in the cell filled with the water-based but non-surfactant and thus non-toxic lyotropic chromonic liquid crystal (LCLC). The LCLC molecules have a plank-like rigid aromatic core and ionic groups at the periphery. Their face-to-face stacking in water produces elongated aggregates-rods that form the nematic phase [10]. Small and isolated particles do not disrupt the uniform alignment of LCLC (which is achieved by techniques [11] similar to the LC display industry standards) but the formation and growth of immune complexes trigger director distortions detectable by optical means (Fig. 1).

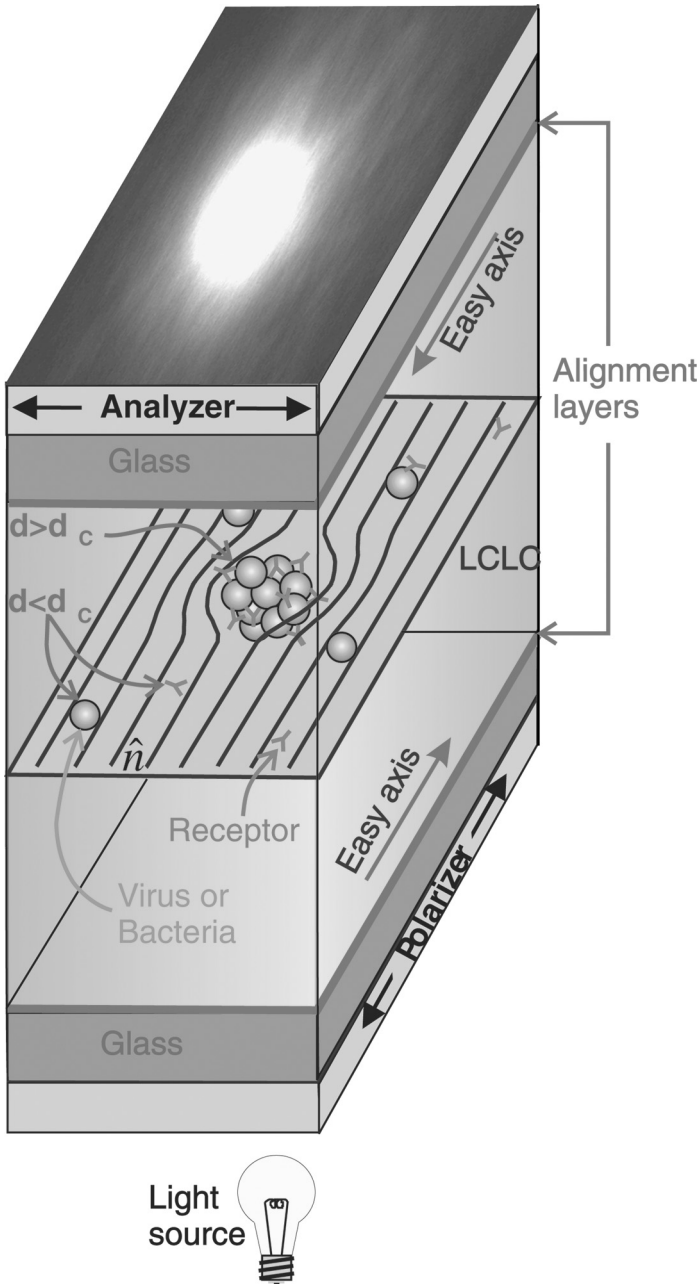

FIGURE 1 The scheme of the lyotropic chromonic liquid crystal biosensor for the detection and amplification of immune complexes.

As the physical model, we consider a spherical particle embedded in the LCLC bulk which sets a tangential orientation of **n**; this geometry is studied much less than the case of normal anchoring [12–14]. Tangential orientation of LCLC at most interfaces is caused by the ionic groups at the lateral surface of the rods. We calculate the distortions as the function of the particle's size and the anchoring strength and demonstrate that the transmission of polarized light through the system increases dramatically with the particle size. This model describes well the experimental data obtained with spherical antigen-coated (streptavidin) latex beads that are aggregated into complexes by anti-streptavidin antibodies.

THEORY

Structure

To find a director field around a spherical particle one should minimize the Frank–Oseen free energy functional and the surface energy. The Frank–Oseen energy of director distortions reads:

$$F_{FO} = \int \begin{bmatrix} \frac{K_{11}}{2}(\text{div } \mathbf{n})^2 + \frac{K_{22}}{2}(\mathbf{n} \text{ curl } \mathbf{n})^2 + \frac{K_{33}}{2}[\mathbf{n} \times \text{curl } \mathbf{n}]^2 \\ -K_{24}\text{div } (\mathbf{n} \text{ div } \mathbf{n} + \mathbf{n} \times \text{curl } \mathbf{n}) \end{bmatrix} dV, \quad (1)$$

where K_{11}, K_{22}, K_{33}, and K_{24} are the Frank elastic constants. Note that the divergence K_{24} term will give non-zero contribution.

The energy of the tangential anchoring at the particle surface is calculated in the Rapini–Papoular approximation

$$F_s = \frac{1}{2}\int \mathrm{W}(\mathbf{n}\boldsymbol{\gamma})^2 \mathrm{dS}, \quad (2)$$

with $\boldsymbol{\gamma}$ being the unit vector normal to the particle surface. An axial symmetry allows us to describe the director field in the spherical coordinate system $\{\mathrm{r}, \theta, \varphi\}$ by the single distortion angle $\beta(\mathrm{r}, \theta)$ between the director and undistorted direction, Figure 2. Note that in the spherical coordinate system $\mathbf{n} = \{\cos(\beta + \theta), -\sin(\beta + \theta), 0\}$.

We use an approximation ($\mathrm{K}_{11} = \mathrm{K}_{33} = \mathrm{K}$) and the K_{22} term does not contribute.

$$F_{tot} = \frac{K}{2}\int \left[\left(\frac{\partial\beta}{\partial r}\right)^2 + \left(\frac{1}{r}\frac{\partial\beta}{\partial\theta}\right)^2 + \left(\frac{\sin\beta}{r\sin\theta}\right)^2\right] dV + \frac{1}{2}\int \left[\mathrm{W}\cos^2(\beta - \theta) + \frac{K - 2K_{24}}{R}\left(\frac{\sin\beta}{\sin\theta}\cos(\beta - \theta) + \frac{\partial\beta}{\partial\theta}\right)\right] dS, \quad (3)$$

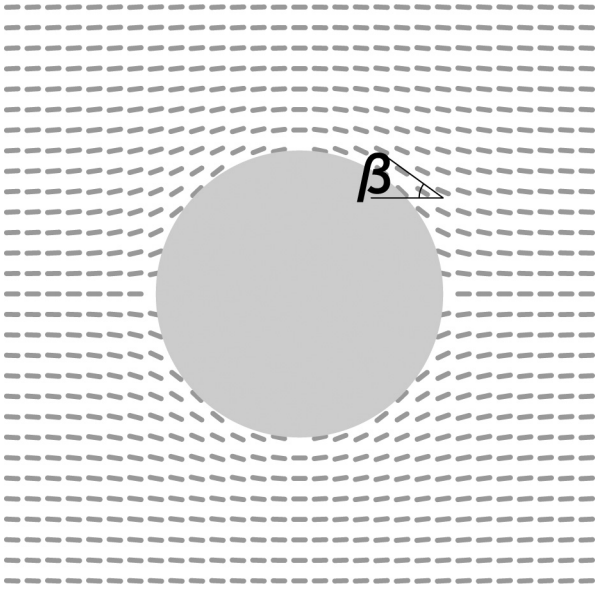

FIGURE 2 Distortions around a spherical particle with tangential anchoring.

From the condition of minimum of $\delta F_{bulk} = 0$ we obtain the equilibrium equation

$$\nabla^2 \beta - \frac{\sin 2\beta}{2\mathrm{r}^2 \sin\theta} = 0. \tag{4}$$

If the particle is small or the anchoring is weak, then $\beta < 1$ and the problem can be linearized. The general solution of the linearized Eq. (4) decaying at infinity is [12]:

$$\beta = \sum_{\mathrm{k}} \frac{\mathrm{C_k}}{\mathrm{r}^{\mathrm{k}+1}} P^1_{\mathrm{k}}(\cos\theta), \tag{5}$$

where $\mathrm{P}^1_{\mathrm{k}}(\cos\theta)$ are the associated Legendre polynomials. The boundary condition at the particle surface selects the mode $\mathrm{k} = 2$ with all other coefficients zero, $\mathrm{C}_{\mathrm{k}\neq 2} = 0$:

$$\beta = \beta_0 \left(\frac{R}{\mathrm{r}}\right)^3 \sin 2\theta, \qquad \beta_0 = \frac{R}{2\left(\xi + \frac{R}{7}\right)} \tag{6}$$

where β_0 is the amplitude of the distortions and $\xi = 2(K + K_{24})/W$ is the anchoring extrapolation length for a spherical particle. The linear approximation used in derivation implies that $\beta_0 < 0.5$, i.e., $R < \xi$.

However Eq. (6) remains a good approximation even for strong anchoring $R > \xi$ assuming that β_0 achieves the saturation value $\pi/4$.

Optics

Calculation of light transmittance through the distorted sample placed between two polarizers is challenging as $\hat{\mathbf{n}}$ changes with respect to the polarization plane. We chose the Cartesian coordinate system $\{x, y, z\}$ with the origin at the particle center, z-axis normal to the substrates, and x-axis along the rubbing direction at the plates, so that $\hat{\mathbf{n}} = \{\cos\beta, -y/\sqrt{y^2+z^2}\sin\beta, -z/\sqrt{y^2+z^2}\sin\beta\}$. Although the amplitudes of polar n_z and azimuthal n_y distortions are approximately equal, their influence on the transmitted intensity is different, with n_y being a major factor, whereas n_z causing only a slight change of the effective extraordinary index. Therefore, we neglect the polar distortions and assume $\hat{\mathbf{n}} = \{\cos\Theta, \sin\Theta, 0\}$, where the rotation angle Θ is derived from Eq. (6):

$$\Theta = \frac{-\beta_0 \rho^2 R^3 \sin 2\Phi}{(\rho^2 + z^2)^{5/2}}; \tag{7}$$

$\rho = \sqrt{x^2+y^2}$ and $\Phi = \tan^{-1}(y/x)$.

Several approaches have been used to describe light propagation through inhomogeneous birefringent media. If the azimuthal angle of the optical axis Θ is constant, then there is no interaction between ordinary and extraordinary waves and the transmitted intensity is determined by the well-known expression for polarized light microscopy, see, e.g., Ref. [8]. When the director rotation in the xy plane is slow, one can describe the light propagation with ordinary and extraordinary waves in a rotating frame $O\xi\eta z$ ($\hat{\mathbf{e}}_\eta \perp \hat{\mathbf{n}}$) and consider the wave transformation as a perturbation caused by the frame rotation with a perturbative parameter $\mu = L\Theta'$, where $L = \lambda/(2\pi|\Delta n|)$ is the retardation length, $\Delta n = n_e - n_o$ is birefringence, λ is the wavelength in vacuum, and prime means the z derivative [15,16]. We use an alternative approach, taking the exact solutions of the wave equation in a cholesteric-like helical structure with a homogeneous rotation $\Theta' = const$ as the non-perturbed solutions. In the rotating frame $O\xi\eta z$ such a solution for the forward waves reads:

$$\begin{aligned}\tilde{\boldsymbol{E}} = {} & A_1(\cos\alpha_1\hat{\mathbf{e}}_\xi + i\sin\alpha_1\hat{\mathbf{e}}_\eta)\exp\{i\Psi_1\} \\ & + A_2(i\sin\alpha_2\hat{\mathbf{e}}_\xi + \cos\alpha_2\hat{\mathbf{e}}_\eta)\exp\{i\Psi_2\}\end{aligned} \tag{8}$$

where $\Psi_j(z) = \int_{z_0}^{z} q_j d\tilde{z}$ is the phase of the jth wave with the wavevector q_j and the ellipticity α_j that depend on Θ', and z_0 is the

coordinate of the input boundary of the LC layer. The inhomogeneity of rotation is a perturbation that affects the amplitudes A_j. Assuming that the rotation inhomogeneity is smooth, $|\Theta'|\lambda < 1$, one can neglect the coupling between forward and backward waves and derive the following equations:

$$\begin{aligned}\cos(\alpha_1-\alpha_2)A_1' &= \sin(\alpha_1-\alpha_2)\alpha_1' A_1 - i\exp\{-i\Delta\Psi(z)\}\alpha_2' A_2\\ \cos(\alpha_1-\alpha_2)A_2' &= \sin(\alpha_2-\alpha_1)\alpha_2' A_2 - i\exp\{i\Delta\Psi(z)\}\alpha_1' A_1\end{aligned} \tag{9}$$

where $\Delta\Psi(z) = \Psi_1(z) - \Psi_2(z)$ is the phase retardation between the two waves. The relative birefringence is small, $\delta = (n_e - n_o)/(n_e + n_o) = -0.006$ for a LCLC used in this work [17]. Thus when $|\Theta'|\lambda < 1$, we can use the approximate expressions for $q_j \approx \kappa \pm \kappa\delta\sqrt{1+\mu^2}$ and $\alpha_j \approx \alpha = \frac{1}{2}\tan^{-1}\mu$ in Eq. (10) with accuracy better than 1%. Here $\kappa = \pi(n_e + n_o)/\lambda$ and $\mu = \Theta'/(\kappa|\delta|)$ coincides with the definition above. The effect of deviation of the light propagation direction from the normal on integrated transmitted intensity I_t, caused by distortions around a particle, is negligibly small. Thus,

$$I_t = I_0 \int_R^\infty \rho d\rho \int_0^{2\pi} d\Phi |t|^2 \tag{10}$$

is expressed through the transmittance coefficient $t = \hat{\mathbf{P}}_\mathbf{A} \cdot \mathbf{S}_2^{-1}\mathbf{T}\mathbf{S}_1\hat{\mathbf{P}}_\mathbf{P}$, where $\hat{\mathbf{P}}_{P(A)}$ is the unit vector defining the orientation of polarizer (analyzer), $\mathbf{T}$ is the 2×2 transmission matrix in the LC, so that $\tilde{\boldsymbol{A}}_i(z_0+h) = T_{ij}\tilde{\boldsymbol{A}}_j(z_0)$, where $\tilde{\boldsymbol{A}}_i(z) = A_i(z)\exp\{i\Psi_i(z)\}$, and $\mathbf{S}_k = \begin{pmatrix} \cos\alpha^{(k)} & -i\sin\alpha^{(k)} \\ -i\sin\alpha^{(k)} & \cos\alpha^{(k)} \end{pmatrix}$ is the matrix that determines the transformation between tangential components of the electric field, which are parallel and perpendicular to the director, and $\tilde{\boldsymbol{A}}_j$ at the boundaries between LC and input (k = 1) or output (k = 2) substrates; here $\alpha^{(k)}$ is the ellipticity at the kth boundary.

To increase the signal/background ratio we use the scheme with crossed polarizers where the polarizer is along easy axis at the substrates. For this scheme $|t|$ at the first perturbation order reads.

$$\begin{aligned}|t| = \Bigg|\Theta_1 - \Theta_2\exp\{i\overline{\Delta\Psi}\} + \frac{1}{L}\int_{z_0}^{z_0+h} \tan^{-1}\mu\sqrt{1+\mu^2}\\ \times\exp\{i\Delta\Psi(z)\}dz\Bigg|.\end{aligned} \tag{11}$$

where $\Theta_{1(2)}$ is the angle between $\hat{\mathbf{n}}$ and the easy axis at the input (output) boundary.

The energy of distortions around the particle is minimal if the particle is in the middle plane of cell [18].

If $h \gg R$, $\Theta_{1,2} = 0$ and

$$|t| = \frac{2}{L}\int_0^\infty \tan^{-1}\mu\sqrt{1+\mu^2}\,\sin\Delta\Psi_0(z)dz, \tag{12}$$

where $\Delta\Psi_0(z) = L^{-1}\int_0^z \sqrt{1+\mu^2}d\tilde{z}$ is the phase retardation between the waves with respect to the particle's z coordinate. Expanding $|t|$ with respect to $c = \beta_0 R^3 L \sin 2\Phi/\rho^4$, one obtains $|t| = c\nu^4/3(\mathrm{K}_2(\nu))$, where $\nu = \rho/L$ and $\mathrm{K}_m(\nu)$ is the modified Bessel function of the order m. Substituting $|t|$ in (11) we obtain the final expression:

$$I_t = I_0\frac{\pi\beta_0^2 R^2 a^6}{9}\{\mathrm{K}_1(a)\mathrm{K}_3(a) - \mathrm{K}_2^2(a)\} \tag{13}$$

where $a = R/L$. The dependence $I_t(R)$ is steep: $I_t(R) \propto R^6$ for weak anchoring at the particle's surface and $I_t(R) \propto R^4$ for strong anchoring when β_0 is constant.

EXPERIMENT

The nematic LCLC was formed by (12–14.5) wt.% solutions of disodium cromoglycate (DSCG, Spectrum Chemical Mfg Corp) in deionized water. We evaluated the toxicity of LCLC with respect to the bacterium E. coli. Live bacteria were placed in the LC samples for 15–60 min, then washed, sub-cultured onto nutrient agar, incubated 24–48 hr and then evaluated for growth. The treatment with DSCG had no effect on viability of the bacteria. In contrast, E. coli ceased to grow after the similar treatments with surfactant lyotropic LC formed by the mixture of cetylpiridimium chloride (2.5–12.5 wt%), hexanol (2.5–12.5 wt%) and brine (95–75 wt%).

We used fluorescent-labelled (Dragon Green fluorochrome), antigen-coated (streptavidin) latex beads (Bangs Laboratories, Inc.) of diameter d =0.56 μm. An anti-streptavidin antibody (1.0 mg/mL; Rockland, Inc.) contained the fluorescent label. The beads (concentration 10^6–10^7 per mL) were added to the LCLC so that the final concentration of DSCG in water was 13 wt%. In a similar way, the antibodies were added (0.01–1.0 mg/mL) to LCLC. The two mixtures were combined in equal proportions to create immune complexes in 13 wt% solution of DSCG. The LCLC mixtures with beads and antibodies only served as control samples. The glass plates coated with rubbed polyimide SE-7511 (Nissan Chemical, Japan) set a planar alignment of LCLC. The sample was formed by two such plates separated by Mylar spacers (3 M) of

variable thickness in the range 8–30 μm; the specimens were sealed with epoxy glue.

All samples were evaluated 30 min after the preparation under the microscope BX-50 Olympus capable of two methods of observation, a regular polarized microscopy to evaluate light transmittance $I_t(R)$ and the fluorescence microscopy to identify the labelled beads, Figure 3A, C, E. The polarising microscopy of the same regions, Figure 3B, D, F clearly demonstrated that the intensity of transmitted light I_t strongly depends on the size of complexes. The individual non-reacted beads and antibodies and complexes smaller than 2 microns in diameter did not cause any noticeable light transmission through the crossed polarizers and the LCLC sample, $I_t \approx 0$, Figure 2B. In contrast, complexes larger than $d_c \approx 2\,\mu\text{m}$ produced noticeable light transmission, Figure 4, caused by director distortions in the surrounding LCLC matrix, Figure 2D, F, over the area much larger than the complexes themselves (compare Fig. 2E and 2F). In control samples, non-reacted antibodies and antigens did not cause noticeable light transmittance in polarising-microscope observations.

Figure 3 demonstrates that the intensity of transmitted light increases with the radius of complexes once the complexes become larger than $R_c \approx 1\,\mu\text{m}$. Each data point represents an immune complex that was first detected and characterised by fluorescence microscopy. The (average) complex diameter was measured using an eyepiece micrometer. Then the polarising-microscope mode was used to measure and normalise the intensity of light of Kr laser $\lambda = 0.568\,\mu\text{m}$ passing through a $H \times H = 50\,\mu\text{m} \times 50\,\mu\text{m}$ area of LCLC cassette with the identified complex at the centre of it.

The normalised light intensity was determined by the formula $I_N = (I_t - I_b)/(\bar{I}_b - I_b)$, where I_t is the light intensity transmitted through the area with the director distortions caused by the complex, I_b is light intensity transmitted through the same area of an unperturbed (uniform) part of the same sample, and $\bar{I}_b$ is the transmittance through the same uniform area rotated by $\Theta_0 = 5^\circ$ with respect to the polarizer; $\bar{I}_b - I_b = I_0 H^2 \sin^2 2\Theta_0 \sin^2(h/2L) \approx 71\,\mu\text{m}^2$. The quantity I_N is normalised by the uniform bright field and reflects the relative amplitude (angle β) of director distortions.

The experimental data for I_N are fitted with two theoretical curves calculated according to Eq. (13) with $L = 5.65\,\mu\text{m}$. The solid line that corresponds to 'strong' anchoring, where $\beta_0 = const$, produces much better fit than the dashed line calculated for 'weak' anchoring, in which case β_0 is determined by Eq. (6). The fitting coefficient for solid line is approximately four times larger that the value estimated from Eq. (13) with $\beta_0 = \pi/4$. The discrepancy is caused by non-spherical

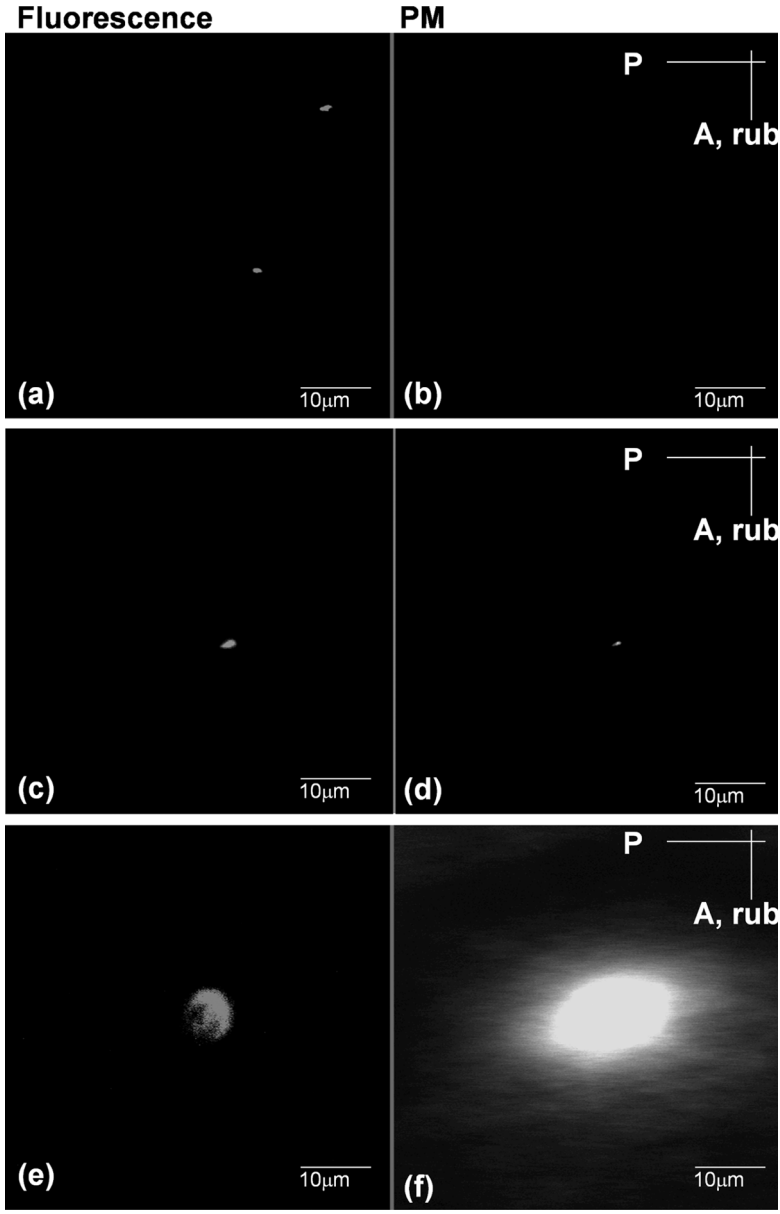

FIGURE 3 The left column shows the fluorescence confocal microscopy textures and the right column shows the corresponding polarising microscopy textures of ligand-coated latex beads (0.56 μm). Small aggregates (A) with $d \leq 2\,\mu m$ did not cause detectable director distortions (B), aggregates of size $d \approx 2\,\mu m$ (C) gave rise to minimally detectable distortions (D), whereas aggregates exceeding 2 μm, (E) caused substantial director distortions readily visualised by polarising microscopy (F).

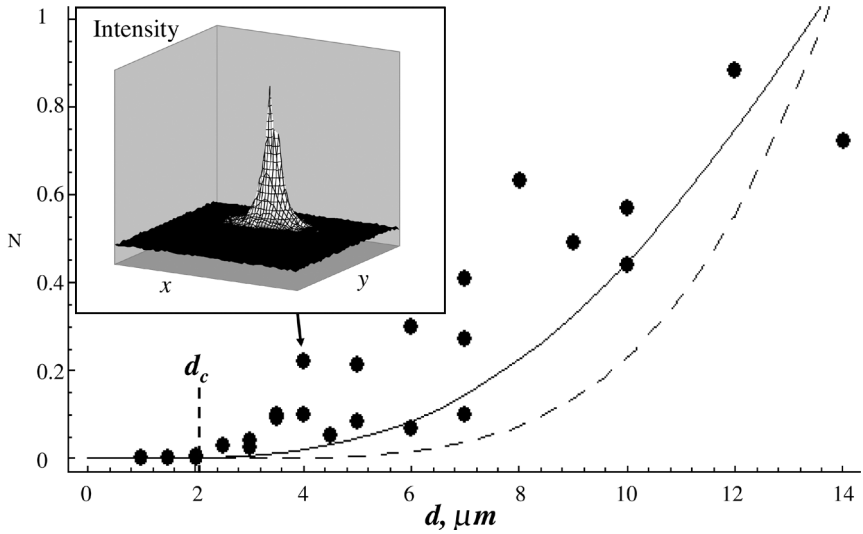

FIGURE 4 Normalised light transmission, I_N, through a 15 μm thick LCLC sample in the polarising-microscope mode as the function of the average diameter of the immune complex. The inset shows the signal intensity created by the $d \approx 4\,\mu m$ aggregate in a $50\,\mu m \times 50\,\mu m$ area of LCLC. The signal amplitude is an order of magnitude higher than the background. The theoretical curves are calculated according to Eq. (13) with $L = 5.6\,\mu m$: solid line is for 'strong' anchoring, $\beta_0 = const$, and the dashed line is for 'weak' anchoring, in which case $\beta_0 \propto d$, Eq. (6).

shape of complexes and the finite cell thickness that results in $\Theta_{1,2} \neq 0$ and finite limits of integration in Eq. (11).

The steep dependence $I_N(d)$ allows one to introduce the critical size d_c, below which I_N can be considered as negligible; d_c depends on material parameters ξ and L, and on the cell thickness h, Eqs. (6, 10–13). The mechanism above fits the microbial detection purpose if the immune complexes are larger than d_c but the individual microbe is smaller than d_c. In our experiments, $d_c \approx 2\,\mu m$; most likely, it can be tuned (for example, by tuning the anchoring length ξ) in the range of (0.1–10) μm, which is the range of interest for microbiological applications. In such a case, microbes and antibodies, being individually too small to perturb $\hat{\mathbf{n}}$, will remain invisible, while immune complexes will be amplified by distortions and brought into evidence by optical transmission. The biological selectivity of detection is guaranteed by the selectivity of antibody-antigen binding. The biosensor would function in real time as determined by

formation of immune aggregates as the director distortion at length scales (0.1–10) μm, occur faster than 0.1 s.

This material is based upon work supported by the National Science Foundation and the Intelligence Technology Innovation Center through the joint "Approaches to Combat Terrorism" Program Solicitation NSF 03-569 (DMR-0346348). We gratefully acknowledge the generous donation by Mrs. Glenn H. (Jessie) Brown in support of this research, partial support by Ohio Board of Regents and Micro-Diagnosis, Inc.

REFERENCES

[1] Gupta, V. K., Skaife, J. J., Dubrovsky, T. B., & Abbott, N. L. (1998). *Science*, *279*, 2077.
[2] Woolverton, C. J., Niehaus, G. D., Doane, K. J., Lavrentovich, O., Schmidt, S. P., & Signs, S. A. (2001). *U.S. Patent 6*, *171*, 802.
[3] Abbott, N. L., Skaife, J. J., Gupta, V. K., Dubrovsky, T., & Shah, R. (2001). *US Patent 6*, *284*, 197.
[4] Fang, J., Ma, W., Selinger, J., & Shashidhar, R. (2003). *Langmuir*, *19*, 2865.
[5] Hoogboom, J., Clerx, J., Otten, M. B. J., Rowan, A. E., Rasing, T., & Nolte, R. J. M. (2003). *Chem. Comm.*, 2856.
[6] Choi, Y., Lee, Y., Kwon, H., & Lee, S. D. (2004). *Materials Science and Engineering*, C *24*, 237.
[7] Brake, J. M., Daschner, M. K., Luk, Y. Y., & Abbott, N. L. (2003). *Science*, *302*, 2094.
[8] Kleman, M. & Lavrentovich, O. D. (2003). *Soft Matter Physics: An Introduction*, Springer, New York, 2003, 638.
[9] Luk, Y.-Y., Campbell, S. F., Abbott, N. L., & Murphy, C. J. (2004). *Liquid Crystals*, *31*, 611.
[10] Lydon, J. (1998). *Current Opin. Colloid & Interface Sci.*, *3*, 458.
[11] Lavrentovich, O. D. & Ishikawa, T. (2002). *US Patent No. 6*, *411*, 354.
[12] Kuksenok, O. V., Ruhwandl, R. W., Shiyanovskii, S. V., & Terentjev, E. M. (1996). *Phys. Rev. E*, *54*, 5198.
[13] Poulin, P., Stark, H., Lubensky, T. C., & Weitz, D. (1997). *Science*, *275*, 1770.
[14] Stark, H. (2001). *Phys. Reports*, *351*, 387.
[15] Allia, P., Oldano, C., & Trossi, L. (1987). *Molec. Cryst. Liq. Cryst.*, *143*, 17.
[16] Faetti, S. & Mutinati, G. C. (2003). *Phys. Rev. E*, *65*, 026601.
[17] Yu. A. Nastishin, Liu, H., Schneider, T., Shiyanovskii, S. V., Lavrentovich, O. D. *et al.*, in preparation.
[18] Voloschenko, D., Pishnyak, O. P., Shiyanovskii, S. V., & Lavrentovich, O. D. (2002). *Phys. Rev. E*, *65*, 060701(R).